Journal of Microbiology (2015) Vol. 53, No. 11, pp. 776–782
DOI 10.1007/s12275-015-5475-8

The crystal structure of the D-alanine-D-alanine ligase from *Acinetobacter baumannii* suggests a flexible conformational change in the central domain before nucleotide binding[§]

Kim-Hung Huynh[1†], Myoung-ki Hong[1†], Clarice Lee[1,2], Huyen-Thi Tran[1], Sang Hee Lee[3], Yeh-Jin Ahn[4], Sun-Shin Cha[5], and Lin-Woo Kang[1*]

[1]*Department of Biological Sciences, Konkuk University, Seoul 143-701, Republic of Korea*
[2]*The Lawrenceville School, Lawrenceville, NJ, USA*
[3]*National Leading Research Laboratory of Drug Resistance Proteomics, Department of Biological Sciences, Myongji University, Yongin 449-728, Republic of Korea*
[4]*Department of Life Science, Sangmyung University, Seoul 110-743, Republic of Korea*
[5]*Marine Biotechnology Research Division, Korea Institute of Ocean Science and Technology, Ansan 426-744, Republic of Korea*

(Received Sep 25, 2015 / Revised Oct 20, 2015 / Accepted Oct 20, 2015)

***Acinetobacter baumannii*, which is emerging as a multidrug-resistant nosocomial pathogen, causes a number of diseases, including pneumonia, bacteremia, meningitis, and skin infections. With ATP hydrolysis, the D-alanine-D-alanine ligase (DDL) catalyzes the synthesis of D-alanyl-D-alanine, which is an essential component of bacterial peptidoglycan. In this study, we determined the crystal structure of DDL from *A. baumannii* (AbDDL) at a resolution of 2.2 Å. The asymmetric unit contained six protomers of AbDDL. Five protomers had a closed conformation in the central domain, while one protomer had an open conformation in the central domain. The central domain with an open conformation did not interact with crystallographic symmetry-related protomers and the conformational change of the central domain was not due to crystal packing. The central domain of AbDDL can have an ensemble of the open and closed conformations before the binding of substrate ATP. The conformational change of the central domain is important for the catalytic activity and the detail information will be useful for the development of inhibitors against AbDDL and putative antibacterial agents against *A. baumannii*. The AbDDL structure was compared with that of other DDLs that were in complex with potent inhibitors and the catalytic activity of AbDDL was confirmed using enzyme kinetics assays.**

***Keywords*:** D-alanine-D-alanine ligase, drug target, bacterial cell wall synthesis, *Acinetobacter baumannii*, X-ray crystallography

[†]These authors contributed equally to this work.
*For correspondence. E-mail: lkang@konkuk.ac.kr; Tel.: +82-2-450-4090; Fax: +82-2-444-6707
[§]Supplemental material for this article may be found at http://www.springerlink.com/content/120956.

Introduction

Acinetobacter baumannii is a nonfermenting Gram-negative coccobacillus. *A. baumannii* has recently emerged as a multidrug-resistant (MDR) pathogen that causes pneumonia, bacteremia, meningitis, and skin infections (Peleg *et al.*, 2008; Sebeny *et al.*, 2008; Howard *et al.*, 2012). In the US alone, of the approximately 12,000 healthcare-associated *Acinetobacter* infections that have been reported by the Centers for Disease Control and Prevention, 63% were MDR (CDC, 2013). The clinical isolates of patients have been shown to confer resistance to most of the currently used antibiotics, including β-lactams, aminoglycosides, macrolides, tetracyclines, phenicols, quaternary amines, streptothricins, sulfonamides, and diaminopyrimidines (Taitt *et al.*, 2014). New targets for MDR pathogens including *A. baumannii* have been searched systematically and D-alanine-D-alanine ligase (DDL; E.C. number 6.3.2.4) is one of the targets.

With ATP hydrolysis, DDL synthesizes the dipeptide D-alanyl-D-alanine (D-ala-D-ala) from two D-alanines (equation 1) (Neuhaus, 1962; Mullins *et al.*, 1990; Fan *et al.*, 1997). D-ala-D-ala is a key component of the bacterial cell wall and it maintains cell wall stability through cross-linking the peptide chain of peptidoglycan. The antibiotic vancomycin, which inhibits the cross-linking of the terminal D-ala-D-ala moiety in the peptide chain of peptidoglycan, is used to treat infections that are caused by methicillin-resistant *Staphylococcus aureus* (Liu *et al.*, 2011). D-Cycloserine (DCS), which is an analog of D-alanine and which was developed as a DDL inhibitor (Neuhaus and Lynch, 1964), was approved for the treatment of Mycobacterium tuberculosis infections. We were interested in determining the crystal structure of AbDDL, which can be used to develop new antibiotic agents against *A. baumannii*.

$$2\ \text{D-alaninest} + \text{ATP} \leftrightarrow \text{D-alanyl-D-alanine} + \text{ADP} + \text{Pi} \quad (1)$$

The structures of DDLs have three domains: the N-terminal, central, and C-terminal domains (Liu *et al.*, 2006; Kitamura *et al.*, 2009; Doan *et al.*, 2014). Loops from each domain, especially the ω-loop and serine-loop, play important roles in the binding of substrates and the catalysis of D-ala-D-ala synthesis. The substrate binding sites for two D-alanines and an ATP exist at the interdomain crevices between the

N-terminal domain and the C-terminal domain and between the central domain and the C-terminal domain, respectively. Four loops from all the three domains complete the substrate binding pocket at the center of the three domains: the loop1 from the N-terminal domain, the loop2 (serine-loop) from the central domain, and the loop3 (ω-loop) and the loop4 from the C-terminal domain. The conformational changes of the three domains and the four loops are closely related to each other and are essential for the catalytic activity of DDL (Kitamura *et al.*, 2009; Doan *et al.*, 2014).

The N-terminal domain and its loop 1 are stable and show little conformational changes during catalysis. The central domain and its serine-loop are highly flexible in the substrate ATP binding. It is still controversial if ATP binding is the first step for the catalytic mechanism of DDL or D-alanine binding is the first step and if the ATP and D-alanine binding is dependent on each other or independent (Bruning *et al.*, 2011; Prosser and de Carvalho, 2013). The conformation of central domain is important for ATP binding (Kitamura *et al.*, 2009). The interdomain conformation of the C-terminal domain is stable like the N-terminal domain, but its ω-loop is mobile depending on substrate nucleotide binding. The ω-loop usually takes a closed conformation with the nucleotide binding and an open flexible conformation without the nucleotide binding. The closed conformation of ω-loop and serine-loop was proposed to play an important role to position the phosphates of ATP for catalysis (Doan *et al.*, 2014).

In this study, we determined the crystal structure of AbDDL with the conformational change of the central domain, which was compared to DDL from *Thermus thermophilus* (TtDDL). In addition, the AbDDL structure was compared with the structures of DDLs that were in complex with other potent inhibitors, including DDL from *S. aureus* (SaDDL) and DDL from *Escherichia coli* (EcDDL). Enzyme kinetics studies of AbDDL were also conducted. An understanding of the crystal structure and conformational change of AbDDL will be useful for determining the catalytic mechanism of AbDDL and developing a new mechanism-based antibiotic agent against *A. baumannii*.

Materials and Methods

Cloning, overexpression, and purification

The cloning of the *AbDDL* gene and the overexpression and purification of AbDDL were performed as previously published (Huynh *et al.*, 2014). Briefly, the *AbDDL* gene was cloned from the genomic DNA of *A. baumannii* OXA-23 to produce a pET11a vector with a 7xHistidine (His) tag at the N-terminus of AbDDL. The resulting pET11a-*AbDDL* recombinant vector was transformed into the *E. coli* strain BL21(DE3)pLysS. The overexpression of AbDDL was induced by adding 0.5 mM isopropyl β-D-1-thiogalactopyranoside when the culture reached an OD_{600} of 0.6 at 310 K. After the induction, the cells were cultured for an additional 4 h. The cultured cells were harvested by centrifugation for 20 min at 6,000 × *g* (Supra 30K A1000S-4 rotors, Hanil Science Industry Corporation) at 277 K. The cell pellets were then resuspended in ice-cold lysis buffer (25 mM Tris-HCl; pH 7.5, 300 mM NaCl, 15 mM imidazole, 3 mM β-mercaptoethanol) and homogenized by ultrasonication on ice (Sonomasher, S & T Science). The lysate was then centrifuged for 40 min at 21,000 × *g* (Vision VS24-SMTi V508A rotor) at 277 K. The supernatant containing soluble AbDDL was loaded onto a Ni^{2+}-charged resin (Ni-NTA His·Bind® Resin, Bio-Rad Laboratories, Inc.) that had been previously equilibrated with the lysis buffer. Affinity purification was performed according to the manufacturer's protocol at 277 K. The lysis buffer was used to wash the nonspecifically bound proteins. AbDDL was eluted with an elution buffer (25 mM Tris-HCl; pH 7.5, 300 mM NaCl, 250 mM imidazole, and 3 mM β-mercaptoethanol). The resulting protein solution was dialyzed for 12 h at 277 K in buffer A (25 mM Tris-HCl; pH 7.5 and 3 mM β-mercaptoethanol). The 7xHis-tag was cleaved with a Tobacco Etch Virus protease at 277 K at a ratio of 20:1 (AbDDL:TEV) by weight in an overnight reaction. The AbDDL without the His-tag was further purified by performing anion exchange chromatography with a Hi-Trap Q FF column (GE Healthcare Life Sciences). The protein was then concentrated to 30 mg/ml in crystallization buffer (25 mM Tris-HCl; pH 7.5, 5 mM NaCl, and 3 mM β-mercaptoethanol) with Vivaspin 20 (10,000 MWCO, Sartorius AG).

Crystallization and X-ray diffraction data collection

The crystallizing conditions were initially applied at 287 K by using the sitting-drop vapor-diffusion method in a 96-well Intelli-Plate (Art Robbins Instruments LLC), the Hydra II e-drop automated pipetting system (Thermo Fisher Scientific Inc.), and screening kits from Crystal Screen Lite, Crystal Screen Cryo, and PEGRx (Hampton Research Corporation), Wizard Precipitant Synergy (Rigaku Reagents, Inc.), and Morpheus MD (Molecular Dimensions Limited). We developed several different crystallization conditions for the AbDDL protein. The first condition (condition 1) was 0.06 M $MgCl_2$ and $CaCl_2$; 0.1 M imidazole; 2-(N-morpholino) ethanesulfonic acid-HCl, pH 6.5; and 30% of the precipitant EDO-P8K containing 40% (v/v) ethylene glycol and 20% (w/v) polyethylene glycol (PEG) 8000 (Huynh *et al.*, 2014). The additional condition (condition 2), which was obtained with the microbatch method in the 72-well MicroWell Mini Trays w/lids (NUNC™), was 0.2 M NaSCN and 20% (w/v) PEG 3350. In both conditions, the fully grown crystals were flash-cooled in liquid nitrogen with cryoprotectant solutions that consisted of each reservoir solution plus 20% (v/v) glycerol. The X-ray diffraction data for the crystals were collected for the 7A and 5C beamlines with the charge-coupled device detectors of an ADSC Quantum 270 and an ADSC Quantum 315r, respectively, at the Pohang Accelerator Laboratory, Pohang University of Science and Technology, South Korea.

Structure determination and refinements

The structure of AbDDL in crystallization condition 1 was determined with the molecular replacement program of Phaser-MR from the CCP4 software package (Winn *et al.*, 2011), and the DDL from *Yestis pestis* was used as a template model (Protein Data Bank [PDB] ID: 3v4z). The AbDDL

Table 1. Data-collection and refinement statistics

Data collection		
X-ray source	7A, PLS	5C, PLS
Wavelength (Å)	0.97935	0.97960
Space group	$P2_12_12_1$	$C2$
Unit-cell parameters		
a, *b*, *c* (Å)	113.4, 116.7, 176.6	221.6, 74.8, 143.1
α, β, γ (°)	90.0, 90.0, 90.0	90.0, 103.3, 90.0
Resolution (Å)	50.00–2.80 (2.85–2.80)	50.00–2.20 (2.24–2.20)
Total reflections	413163	599505
Unique reflections	55982	115881
Completeness (%)	96.0 (92.0)	99.6 (99.0)
Multiplicity	7.4 (3.7)	5.2 (4.1)
$\langle I/\sigma(I)\rangle$	12.9 (1.6)	22.1 (2.1)
R_{merge} (%)	9.1 (42.0)	9.7 (52.4)
Refinement		
Resolution (Å)	44.82–2.81	36.05–2.20
No. of reflections	54678	109440
R_{work} / R_{free} (%)	24.8/ 29.3	22.0 / 28.0
No. of atoms		
Protein	11162	12700
Water	69	199
RMSDs		
Bond lengths (Å)	0.013	0.014
Bond angles (°)	1.764	1.755
Ramachandran plot (%)		
Favored	96.4	95.2
Allowed	2.2	4.3
Disallowed	1.4	0.5
PDB accession code	5DMX (crystallization condition 1)	5D8D (crystallization condition 2)

The values in parentheses represent the highest resolution shell.
$R_{merge} = \sum_{hkl} \sum_i |(I_i(hkl)) - \langle I(hkl)\rangle| / \sum_{hkl} \sum_i I_i(hkl)$, where $I_i(hkl)$ is the mean intensity of the *i*th observation of the symmetry-related reflections *hkl*. $R_{free} = \sum_{hkl} ||F_{obs}| - |F_{calc}|| / \sum_{hkl} |F_{obs}|$, where F_{calc} is the calculated protein structure factor in the atomic model (R_{free} was calculated with 5% of randomly selected the reflections).
PDB: protein data bank; RMSD: root mean square deviation.

structure in crystallization condition 2 was determined with the AbDDL structure determined in crystallization condition 1. The model building was performed with the Coot software (Emsley *et al.*, 2010). The resulting structure was refined with Refmac5 of the CCP4 package (Murshudov *et al.*, 2011). The resulting structures were validated in the PROCHECK software (Laskowski *et al.*, 1993). The statistics of the structure refinement are summarized in Table 1. The graphic presentation was performed in the Pymol software (Schrodinger, 2010), and the sequence alignment was performed in ClustalX (Thompson, 1997) and presented with ESPript Server (Gouet *et al.*, 1999).

Enzymatic activity assay

The enzymatic activity of AbDDL was determined by measuring the D-alanine-dependent orthophosphate (Pi) release from ATP, which was detected by the colorimetric method. The assay solution of 50 µl contained 50 mM Tris-HCl (pH 7.8), 10 mM $MgCl_2$, 10 mM KCl, and ATP and D-alanine at required concentrations. The reaction was initiated by the addition of 1.5 µg of the AbDDL enzyme into the assay solution, which was incubated for 10 min. The reaction was stopped by adding 10 mM of ethylenediaminetetraacetic acid and 250 µl of water. The Ames solution (750 µl) was added, and the mixture was incubated at 45°C for 20 min to allow color development. The concentration of released Pi was measured by spectrometry at 820 nm. The kinetic parameters were determined with a nonlinear regression and the following equations (1–3) as described previously (Doan *et al.*, 2014). The basic equation (equation 2) for DDL was derived from the steady state kinetics for two identical substrate molecules of D-alanine. To obtain the K_{cat} and K_{m2} values for the D-ala-D-ala ligase activities, equation 3 was used. K_{m1} was calculated with equation 4. To calculate the K_{cat} for ATP and $K_{m,ATP}$, we used the steady-state kinetics of the Michaelis-Menten equation with a single binding site. To test the inhibitory effects of DCS on AbDDL, the fixed concentrations of 5 mM or 10 mM of DCS were added into the assays with the various concentrations of D-alanine or ATP.

$$\frac{1}{v} = \frac{1}{V_{max}} + \frac{K_{m2}}{V_{max}}\frac{1}{[S]} + \frac{K_{m1}K_{m2}}{V_{max}}\frac{1}{[S]^2} \quad (2)$$

$$\frac{1}{v} = \frac{1}{V_{max}} + \frac{K_{m2}}{V_{max}}\frac{1}{[S]} \quad (3)$$

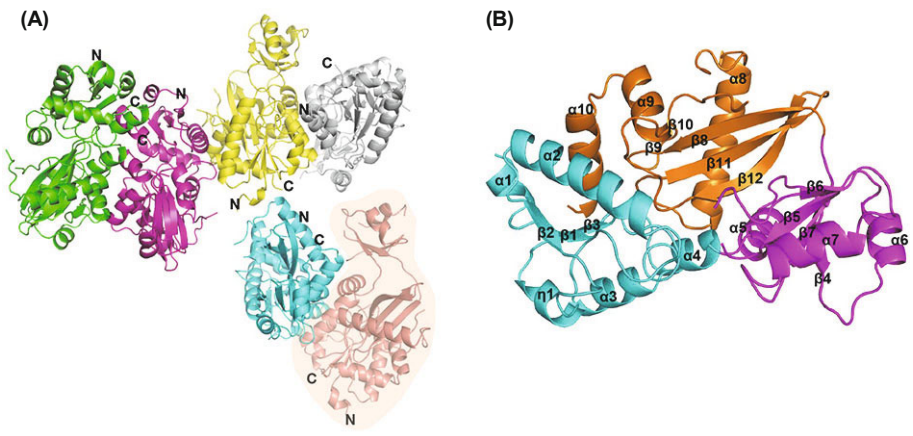

Fig. 1. The crystal structure of the *A. baumannii* D-alanine-D-alanine ligase (AbDDL). (A) Six protomers (three dimers) are shown in the asymmetric unit. The protomer with the open conformation of the central domain is shaded in salmon. N-terminus and C-terminus of each protomer is labelled. (B) Three domains are shown in the AbDDL protomer. The N-terminal, central, and C-terminal domains are shown in cyan, purple, and orange, respectively.

$$[S]\left(\frac{1}{v}-\frac{1}{V_{max}}\right)=\frac{K_{m2}}{V_{max}}+[S]\frac{K_{m1}K_{m2}}{V_{max}} \quad (4)$$

Results

Overall structure

The AbDDL protein was purified to the level of a single band on sodium dodecyl sulfate-polyacrylamide gel electrophoresis and exists as a dimer according to the results of the size exclusion chromatography. The crystal structures of AbDDL were determined at 2.8 Å and 2.2 Å resolutions by molecular replacement in two different crystallization conditions. In the first crystallization condition (Huynh *et al.*, 2014), all the AbDDL protomers showed the same overall conformation. However, in the second condition, where six protomers were observed in an asymmetric unit (Fig. 1A), one of the six protomers showed the conformational change in central domain. When the protomer structures from both crystallization conditions were compared, the structures were well conserved (the root-mean-square deviation is 0.34 Å for 228 residues in 303 residues), except the one promoter with the conformational change in the second condition (Supplementary data Fig. S1A).

We focused on the AbDDL structure in the second condition. The geometry and stereochemistry of the determined AbDDL structure were good and 95% of the residues were in the most favored region of the Ramachandran plot. The data collection and refinement statistics are summarized in Table 1.

The overall structure of AbDDL consisted of the N-terminal, central, and C-terminal domains, which were well conserved in DDLs (Fig. 1B). The main scaffold of all three of the domains was an α/β fold of a tightly folded globular shape. The N-terminal domain and central domain were connected with two consecutive 2 α-helices that were arranged linearly and that were bound beneath the C-terminal domain. The three resulting domains were closely bound to each other. The C-terminal domain had a conserved ω-loop, the conformation of which is known to change depending on substrate nucleotide binding (Kitamura *et al.*, 2009). The ω-loop of AbDDL was disordered in all the six protomers due to its flexibility when nucleotides were not bound and this is frequently observed in other DDLs (Wu *et al.*, 2008; Doan *et al.*, 2014). The serine-loop in the central domain also showed flexible conformations.

The conformational change in the central domain

In the TtDDL structure (36% sequence identity with AbDDL), the central domain showed gradual conformational changes relative to substrate nucleotide binding (Kitamura *et al.*, 2009). We superimposed six AbDDL protomers with each other in order to examine the conformational differences. Although the central domain of five AbDDL protomers showed the closed conformation, the central domain of one protomer was tilted by 33° by rolling around the surface of the C-terminal domain, which resulted in a wide-open substrate nucleotide-binding channel between the central and C-terminal domains (Fig. 2). The conformational change of the central domain was not dependent on substrate nucleotide binding. The open central domain only interacted with the physio-

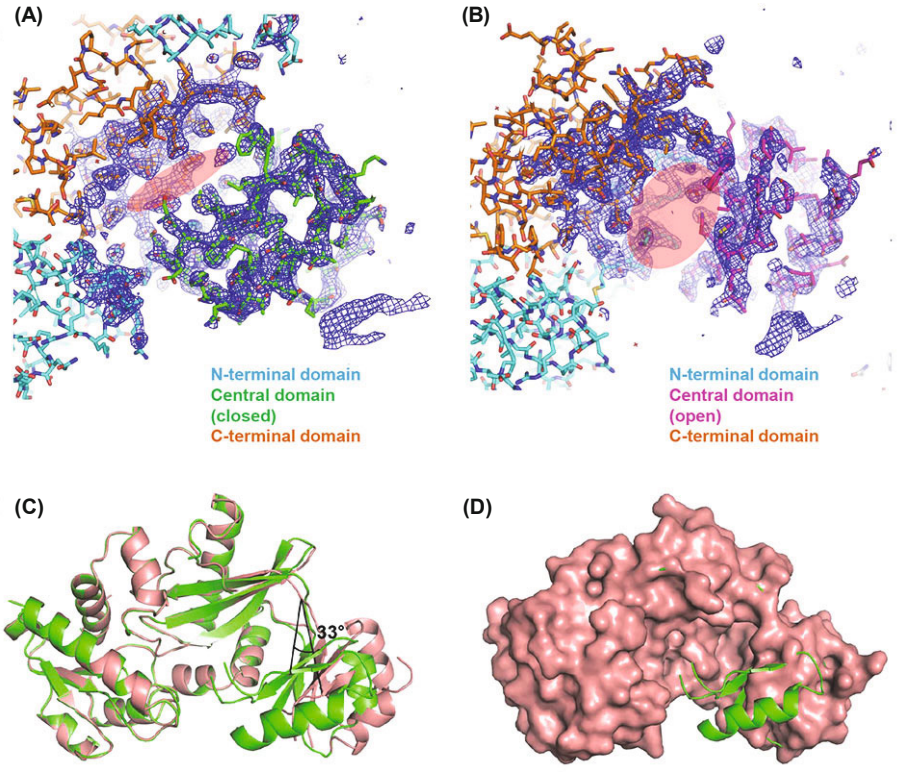

Fig. 2. The closed and open conformations of the central domain. (A) The closed conformation of the central domain. (B) The open conformation of the central domain. The blue mesh shows a 2Fo-Fc map (contoured at 1.0 σ). The cyan color shows the N-terminal domain and the orange color shows the C-terminal domain. The green color shows the closed conformation of the central domain and the purple color shows the open conformation of the central domain. The red oval represents the conserved nucleotide-binding site. (C) The superimposed AbDDL protomers of the open and closed conformations of the central domain. (D) The open conformation of the AbDDL structure is represented as the surface. The closed conformation of AbDDL is the same as (C).

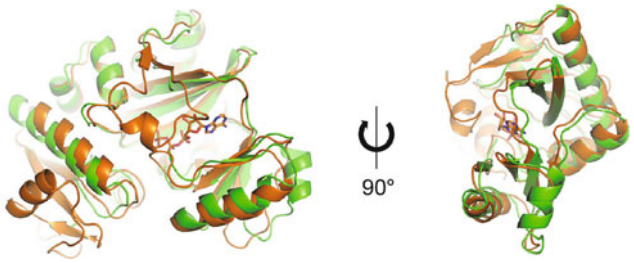

Fig. 3. The ATP binding site of AbDDL. The superimposed structures of the closed conformation of AbDDL (green) and the DDL from *T. thermophilus* (TtDDL; orange) in complex with D-alanyl-D-alanine (D-ala-D-ala) and ATP. The ATP molecule is positioned based on the superimposed TtDDL structure. The ATP molecule in the TtDDL structure is represented as a stick.

Table 2. Enzyme kinetic parameters of the D-alanine-D-alanine ligases (DDLs)

	Km_1 (mM)	Km_2 (mM)	$Km_{,ATP}$ (mM)	kcat (min^{-1})	kcat/Km_2 (mM/min)
AbDDL	0.008	2.7	1.7	1805	669
EcDDLB (Zawadzke *et al.*, 1991)	0.0087	1.26	0.0394	1170	929
XoDDL (Doan *et al.*, 2014)	0.021	12		903	73.3
HpDDL (Wu *et al.*, 2008)	1.89	627	0.87	115	0.18

Ec, *E. coli*; Yp, *Yersinia pestis*; Xo, *Xanthomonas oryzae* pv. oryzae; Sa, *Staphylococcus aureus*; Tt, *Thermus thermophilus*; Hp, *Helicobacter pylori*

logical dimer molecule and did not contact other crystallographic symmetry-related AbDDL molecules (Supplementary data Fig. S2). The conformational change did not result from crystal packing. The central domain was connected to the N-terminal and C-terminal domains through two parallel loops. The loop that was entering into the central domain consisted of six residues, and the loop that was coming out of the central domain consisted of three residues. The center residue (Ile179) of the outgoing loop was the pivotal point for the open and closed conformational changes of the central domain.

The nucleotide-binding site

The interdomain crevice between the central domain and the C-terminal domain contained the conserved nucleotide-binding site. We compared the open and closed conformations of the AbDDL protomer structures. The open conformation of the central domain exposed the large solvent-accessible nucleotide-binding pocket at the bottom of AbDDL, which was unavailable in the closed conformation.

We superimposed the ATP and D-ala-D-ala-bound TtDDL structure on the AbDDL structures in order to examine the nucleotide-binding site (Fig. 3). The superimposed ATP fit well in the crevice between the C-terminal and central domains in the closed conformation of AbDDL without bumping (Supplementary data Fig. S1B). In the open conformation of AbDDL, the bound ATP could not be recognized or interacted with the central domain. The ω-loop was also an important flexible component of the DDLs. The ω-loop of the closed conformation of TtDDL covered the bound ATP completely, and the ATP molecule was not accessible by the solvent except through the small hole near the adenine part of ATP. The three phosphates and the ribose ring were totally covered inside the TtDDL protein. In the closed con-

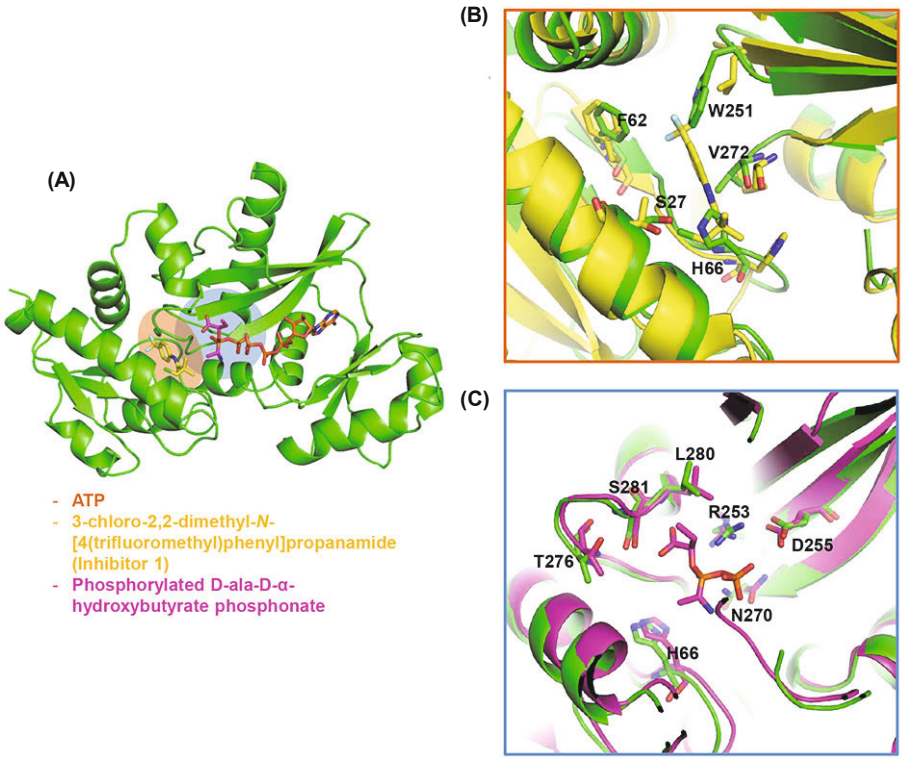

Fig. 4. The comparison of the proposed binding sites of known DDL inhibitors. (A) The putative binding sites of known DDL inhibitors in AbDDL, based on the superimposition of the closed AbDDL structure and the inhibitor-bound DDL structures. ATP (orange), 3-chloro-2,2-dimethyl-*N*-[4(trifluoromethyl)phenyl]propanamide (inhibitor 1) (yellow in the orange shaded oval), and phosphorylated D-ala-D-α-hydroxybutyrate phosphonate (purple in blue shaded circle) are positioned on the closed conformation of the AbDDL structure. (B) The binding site for inhibitor 1 is enlarged in the orange rectangular box, in which the superimposed DDL from *S. aureus* (SaDDL) is shown in yellow. (C) The binding site for phosphorylated D-ala-D-α-hydroxybutyrate phosphonate is enlarged in the blue rectangular box, in which the superimposed DDL from *E. coli* (EcDDL) is shown in purple.

formation of AbDDL, the ω-loop was disordered and it was not visualized because of the flexible conformations. The phosphates, ribose ring, and base of ATP were exposed to the solvent. However, even without the ω-loop, the nucleotide-binding site of AbDDL in the closed conformation was too narrow and tight for nucleotide to bind. Accordingly, the flexible open and closed conformations of the central domain will be important for ATP binding.

The enzyme kinetics assay

We performed an enzyme kinetics assay of AbDDL (Table 2 and Supplementary data Fig. S3). The K_m values for two different substrates, the D-alanines and ATP, were measured in three separate reactions. The K_{m1} value for the first D-alanine (D-ala$_1$) was 0.008 mM and the K_{m2} value for the second D-alanine (D-ala$_2$) was 2.7 mM. Both K_m values of AbDDL for D-ala$_1$ and D-ala$_2$ were slightly higher than that of EcDDL (Zawadzke *et al.*, 1991) and much lower than those of XoDDL and HpDDL (Wu *et al.*, 2008; Doan *et al.*, 2014). The k_{cat} value of AbDDL was higher than those of all compared DDLs. The resulting catalytic efficiency (k_{cat}/K_{m2}) of AbDDL was similar to that of EcDDL. The $K_{m,ATP}$ value of AbDDL was 1.7 mM. We tested if DCS inhibits AbDDL in the same assay condition which is the known inhibitor against DDL from *Mycobacterium tuberculosis* and a tuberculosis drug (Supplementary data Fig. S3). There is no DCS-bound DDL structure available now. Although DCS can inhibit AbDDL in the enzyme assay, the required inhibitory concentration of DCS was as high as the range of mM.

Structural comparisons with potent inhibitor-bound DDLs

To date, many efforts have been made to develop DDL inhibitors with structure-based drug design and molecular docking (Kovac *et al.*, 2007, 2008; Sova *et al.*, 2009; Tytgat *et al.*, 2009; Skedelj *et al.*, 2012; Prosser and de Carvalho, 2013). However, only two different types of inhibitors were determined as cocrystal structures with DDL by X-ray crystallography (Fig. 4). The crystal structure of *S. aureus* DDL (SaDDL) in complex with 3-chloro-2,2-dimethyl-*N*-[4(trifluoromethyl)phenyl]propanamide (inhibitor 1) was determined, and its Ki was 4 μM against SaDDL (Liu *et al.*, 2006). The binding site of inhibitor 1 differed from the substrate-binding site, which was located adjacent to the D-ala binding site. Inhibitor 1 was able to indirectly inhibit D-alanine binding rather than directly competing for the same D-alanine binding pocket. When we superimposed the inhibitor 1-bound SaDDL structure on the AbDDL structure, the corresponding binding site for inhibitor 1 was not found in AbDDL because of the bulkier residues at the binding site.

A different type of inhibitors of D-ala-D-ala phosphinate and D-ala-D-α-hydroxybutyrate phosphonate were shown to bind to *E. coli* DDL (EcDDL) via the D-alanine binding site of EcDDL (Fan *et al.*, 1997). Both inhibitors were transformed to the phosphorylated intermediate form by taking up a phosphate from ATP. The Ki values of the phosphorylated phosphinate intermediate and the phosphorylated phosphonate intermediate for wild-type EcDDL were 33 and 13 nM, respectively. The D-alanine binding site was well conserved in the DDLs and no steric hindrance was observed between the phosphorylated inhibitors and the binding pocket of AbDDL.

Discussion

We soaked the apo-AbDDL crystals in solutions of ATP or an ATP-analog (AMPPNP) in order to determine the nucleotide-bound AbDDL structures. However, we were not able to obtain well-diffracting crystals. In AbDDL structure, the conformational change of the central domain was observed without nucleotide binding and the tilting conformational change (33°) of the AbDDL central domain was much larger than that in TtDDL (14°). The flexible conformational change of the AbDDL central domain can facilitate the easy access of ATP to the binding site. After ATP binds, the closed conformation of the central domain can stabilize the binding interactions between ATP and AbDDL. In addition, the ω-loop closes its conformation to cover the bound ATP tightly. Currently, it is not clear if the closure of the central domain or the closure of the ω-loop comes first. Both conformational changes are the conserved essential steps in the catalytic mechanisms of DDL.

Two different inhibitor-binding pockets have been confirmed previously by X-ray crystallography in SaDDL and EcDDL, and the binding sites were compared in AbDDL. The 3-chloro-2,2-dimethyl-*N*-[4(trifluoromethyl)phenyl]propanamide (inhibitor 1) did not bind at the substrate binding pocket of SaDDL and the equivalent binding site was unavailable in AbDDL. Other inhibitors of the phosphorylated phosphinate and phosphorylated phosphonate bind to the D-alanine-binding site of EcDDL. The parts of EcDDL that interact with the inhibitors consist of all four loops in the active site (Supplementary data Fig. S4). The inhibitor-binding site of the phosphorylated phosphinate and phosphorylated phosphonate is well conserved in AbDDL because the catalytic mechanism is conserved. The inhibitor-binding site is the critical site of connecting three different substrates, the two D-alanines and the ATP, where two consecutive nucleophilic attacks take place between the first D-alanine and ATP and between the phosphorylated first D-ala and the second D-ala. Accordingly, the residues of the inhibitor-binding site and the overall geometry are well conserved in most DDLs and will be a good target position for the development of broad spectrum DDL inhibitors.

In this study, we determined the crystal structure of AbDDL with a conformational change of the central domain and confirmed the enzymatic activity of AbDDL. The conformational change of the central domain can be spontaneous without nucleotide binding. The structural information of AbDDL will be useful for the development of inhibitors against AbDDL and putative antibacterial agents against *A. baumannii*.

PDB ID

AbDDL structure at condition 1: 5DMX
AbDDL structure at condition 2: 5D8D

Acknowledgements

We are grateful to the staff members of Beamline 5C and Beamline 7A in PAL, Republic of Korea. This paper was supported by Konkuk University in 2015.

References

Bruning, J.B., Murillo, A.C., Chacon, O., Barletta, R.G., and Sacchettini, J.C. 2011. Structure of the *Mycobacterium tuberculosis* D-alanine:D-alanine ligase, a target of the antituberculosis drug D-cycloserine. *Antimicrob. Agents Chemother.* **55**, 291–301.

CDC. 2013. Antibiotic resistance threats in the United States: US Department of Health and Human Services Centers for Disease Control and Prevention.

Doan, T.T., Kim, J.K., Ngo, H.P., Tran, H.T., Cha, S.S., Min Chung, K., Huynh, K.H., Ahn, Y.J., and Kang, L.W. 2014. Crystal structures of D-alanine-D-alanine ligase from *Xanthomonas oryzae* pv. *oryzae* alone and in complex with nucleotides. *Arch. Biochem. Biophys.* **545C**, 92–99.

Emsley, P., Lohkamp, B., Scott, W.G., and Cowtan, K. 2010. Features and development of Coot. *Acta Crystallogr. D Biol. Crystallogr.* **66**, 486–501.

Fan, C., Park, I.S., Walsh, C.T., and Knox, J.R. 1997. D-alanine:D-alanine ligase: phosphonate and phosphinate intermediates with wild type and the Y216F mutant. *Biochemistry* **36**, 2531–2538.

Gouet, P., Emmanuel, C., Stuart, D.I., and Métoz, F. 1999. Espript: analysis of multiple sequence alignment in PostScript. *Bioinformatic* **15**, 305–308.

Howard, A., O'Donoghue, M., Feeney, A., and Sleator, R.D. 2012. *Acinetobacter baumannii*: an emerging opportunistic pathogen. *Virulence* **3**, 243–250.

Huynh, K.H., Tran, H.T., Pham, T.V., Ngo, H.P., Cha, S.S., Chung, K.M., Lee, S.H., and Kang, L.W. 2014. Expression, crystallization and preliminary X-ray crystallographic analysis of D-alanine-D-alanine ligase from OXA-23-producing *Acinetobacter baumannii* K0420859. *Acta. Crystallogr. F Struct. Biol. Commun.* **70**, 505–508.

Kitamura, Y., Ebihara, A., Agari, Y., Shinkai, A., Hirotsu, K., and Kuramitsu, S. 2009. Structure of D-alanine-D-alanine ligase from *Thermus thermophilus* HB8: cumulative conformational change and enzyme-ligand interactions. *Acta. Crystallogr. D Biol. Crystallogr.* **65**, 1098–1106.

Kovac, A., Konc, J., Vehar, B., Bostock, J.M., Chopra, I., Janezic, D., and Gobec, S. 2008. Discovery of new inhibitors of D-alanine:D-alanine ligase by structure-based virtual screening. *J. Med. Chem.* **51**, 7442–7448.

Kovac, A., Majce, V., Lenarsic, R., Bombek, S., Bostock, J.M., Chopra, I., Polanc, S., and Gobec, S. 2007. Diazenedicarboxamides as inhibitors of D-alanine-D-alanine ligase (Ddl). *Bioorg. Med. Chem. Lett.* **17**, 2047–2054.

Laskowski, R., MacArthur, M., Moss, D., and Thornton, J. 1993. PROCHECK: a program to check the sterochemical quality of protein structures. *J. Appl. Cryst.* **26**, 283–291.

Liu, C., Bayer, A., Cosgrove, S.E., Daum, R.S., Fridkin, S.K., Gorwitz, R.J., Kaplan, S.L., Karchmer, A.W., Levine, D.P., Murray, B.E., *et al.* 2011. Clinical practice guidelines by the infectious diseases society of america for the treatment of methicillin-resistant *Staphylococcus aureus* infections in adults and children: executive summary. *Clin. Infect. Dis.* **52**, 285–292.

Liu, S., Chang, J.S., Herberg, J.T., Horng, M.M., Tomich, P.K., Lin, A.H., and Marotti, K.R. 2006. Allosteric inhibition of *Staphylococcus aureus* D-alanine:D-alanine ligase revealed by crystallographic studies. *Proc. Natl. Acad. Sci. USA* **103**, 15178–15183.

Mullins, L.S., Zawadzke, L.E., Walsh, C.T., and Raushel, F.M. 1990. Kinetic evidence for the formation of D-alanyl phosphate in the mechanism of D-alanyl-D-alanine ligase. *J. Biol. Chem.* **265**, 8993–8998.

Murshudov, G.N., Skubak, P., Lebedev, A.A., Pannu, N.S., Steiner, R.A., Nicholls, R.A., Winn, M.D., Long, F., and Vagin, A.A. 2011. REFMAC5 for the refinement of macromolecular crystal structures. *Acta. Crystallogr. D Biol. Crystallogr.* **67**, 355–367.

Neuhaus, F.C. 1962. The enzymatic synthesis of D-alanyl-D-alanine. II. Kinetic studies on D-alanyl-D-alanine synthetase. *J. Biol. Chem.* **237**, 3128–3135.

Neuhaus, F.C. and Lynch, J.L. 1964. The enzymatic synthesis of D-alanyl-D-alanine. 3. On the inhibition of D-alanyl-D-alanine synthetase by the antibiotic D-cycloserine. *Biochemistry* **3**, 471–480.

Peleg, A.Y., Seifert, H., andPaterson, D.L. 2008. *Acinetobacter baumannii*: emergence of a successful pathogen. *Clin. Microbiol. Rev.* **21**, 538–582.

Prosser, G.A. and de Carvalho, L.P. 2013. Kinetic mechanism and inhibition of *Mycobacterium tuberculosis* D-alanine:D-alanine ligase by the antibiotic D-cycloserine. *FEBS J.* **280**, 1150–1166.

Schrodinger, L. 2010. The PyMOL Molecular Graphics System, Version 1.3r1.

Sebeny, P.J., Riddle, M.S., and Petersen, K. 2008. *Acinetobacter baumannii* skin and soft-tissue infection associated with war trauma. *Clin. Infect. Dis.* **47**, 444–449.

Skedelj, V., Arsovska, E., Tomasic, T., Kroflic, A., Hodnik, V., Hrast, M., Bester-Rogac, M., Anderluh, G., Gobec, S., Bostock, J., *et al.* 2012. 6-Arylpyrido[2,3-d]pyrimidines as novel ATP-competitive inhibitors of bacterial D-alanine:D-alanine ligase. *PLoS One* **7**, e39922.

Sova, M., Cadez, G., Turk, S., Majce, V., Polanc, S., Batson, S., Lloyd, A.J., Roper, D.I., Fishwick, C.W., and Gobec, S. 2009. Design and synthesis of new hydroxyethylamines as inhibitors of D-alanyl-D-lactate ligase (VanA) and D-alanyl-D-alanine ligase (DdlB). *Bioorg. Med. Chem. Lett.* **19**, 1376–1379.

Taitt, C.R., Leski, T.A., Stockelman, M.G., Craft, D.W., Zurawski, D.V. , Kirkup, B.C., and Vora, G.J. 2014. Antimicrobial resistance determinants in *Acinetobacter baumannii* isolates taken from military treatment facilities. *Antimicrob. Agents Chemother.* **58**, 767–781.

Thompson, J.D., Gibson, T.J., Plewniak, F., Jeanmougin, F., and Higgins, D.G. 1997. The CLUSTAL_X woindows interface:flexible strategies for multiple sequence alignment aided by quality analysis tools. *Nucleic Acids Res.* **25**, 4876–4882.

Tytgat, I., Vandevuer, S., Ortmans, I., Sirockin, F., Colacino, E., Van Bambeke, F., Duez, C., Poupaert, J.H., Tulkens, P.M., Dejaegere, A., *et al.* 2009. Structure-based design of benzoxazoles as new inhibitors for D-alanyl – D-alanine ligase. *Qsar Comb. Sci.* **28**, 1394–1404.

Winn, M.D., Ballard, C.C., Cowtan, K.D., Dodson, E.J., Emsley, P., Evans, P.R., Keegan, R.M., Krissinel, E.B., Leslie, A.G., McCoy, A., *et al.* 2011. Overview of the CCP4 suite and current developments. *Acta Crystallogr. D Biol. Crystallogr.* **67**, 235–242.

Wu, D.L., Zhang, L., Kong, Y.H., Du, J.M., Chen, S.A., Chen, J., Ding, J.P., Jiang, H.L., and Shen, X. 2008. Enzymatic characterization and crystal structure analysis of the D-alanine-D-alanine ligase from *Helicobacter pylori*. *Proteins* **72**, 1148–1160.

Zawadzke, L.E., Bugg, T.D., and Walsh, C.T. 1991. Existence of two D-alanine:D-alanine ligases in *Escherichia coli*: cloning and sequencing of the ddlA gene and purification and characterization of the DdlA and DdlB enzymes. *Biochemistry* **30**, 1673–1682.